Ultra-broadband optical filter based on chirped long-period fiber grating using leaky mode coupling*

XUE Linlin, Bras Samuel Malumba Timoteo, QIU Weiwei, and WANG Zhongpeng**

School of Information and Electronic Engineering, Zhejiang University of Science and Technology, Hangzhou 310023, China

(Received 19 March 2022; Revised 7 June 2022)

An ultra-broadband optical filter was proposed and demonstrated based on leaky mode coupling in a coated chirped long-period fiber grating (CLPFG). The CLPFG was coated with a material whose refractive index (RI) was higher than that of the fiber cladding, enabling the coupling of the core mode to leaky modes, to achieve a desired coupling efficiency. Complex coupled-mode theory was used to investigate the power evolution of the core mode that resulted from the coupling. From this, the conditions in which the core mode power attenuates the most rapidly were identified. In addition, phase matching turning point (PMTP) was used in the design, to overcome the conflict between the range of grating period change and the grating length in the CLPFG. Finally, an optimized CLPFG-based filter with a length of 3.5 cm was obtained, which has a symmetrical attenuation band with an operating bandwidth over 300 nm. Within the operating bandwidth, the flatness is less than 2.5 dB and the transmittance is lower than 0.1%.

Document code: A **Article ID:** 1673-1905(2022)10-0577-6

DOI https://doi.org/10.1007/s11801-022-2039-0

A long-period fiber grating (LPFG) is a type of mode-coupling device, which can couple the light of the core mode to a phased-matched co-propagating cladding mode at a specific wavelength[1,2]. Owing to their advantages of easy fabrication, high isolation and low back-reflection, LPFGs have attracted considerable interest in applications of optical communications and sensing[2,3].

A chirped long-period fiber grating (CLPFG) is a special LPFG which has a varying period along its axis. It retains the advantages of LPFG while has particular properties, so it has attracted many researchers' attention and found important use in broadband filtering, dispersion control, multi-parameter sensing and mode conversion[4-13]. One of the most particular properties of a CLPFG is that it has broader bandwidth compared with that of the LPFG. As the period is varying, the light of the core mode in the CLPFG can couple to the cladding mode in a certain wavelength range, and thus achieving a broad bandwidth[4,10-13]. Normally, a larger period change corresponds to a broader bandwidth. However, for a CLPFG with a constant length, a large period change in the CLPFG would cause a short effective coupling length for each single period, and a short effective coupling length further leads to a low coupling efficiency. Therefore, to obtain high efficiency, a correspondingly long grating would be required, which limits the practical applications of CLPFG-based broadband optical filters[4,10,11]. Recently, ultra-broadband LPFG filters based on phase matching turning point (PMTP) were reported[12,13]. PMTP has been successfully used in sensitivity enhancement of LPFG-based sensors and ultra-broadband mode conversion between LP modes and orbital angular momentum modes of fibers[14-17]. It's known that for a CLPFG-based filter, the slope of its phase matching curves (PMCs) is directly proportional to the broadening speed of its bandwidth, while the slope of PMC at the PMTP reaches the highest. Thus, the using of PMTP could greatly reduce the requirement of grating period change for a broadband design. Although the bandwidth of the CLPFG-based filter was broadened to an ultra-large range, fluctuations on the attenuation band were observed, which strongly influences the filtering performance[12,13]. To eliminate the fluctuations, an apodized CLPFG with Tanh function and Gaussian function was then utilized [12]. However, the apodization may increase the difficulty of fabrication. More importantly, the apodization is hard or even impossible to be implemented in some kinds of fiber gratings, such as chiral fiber grating[18,19]. Therefore, we will focus on an alternative method to achieve an ultra-broadband CLPFG-based optical filter.

In fact, the fluctuations on the attenuation band of the CLPFG-based filter were caused by the periodic

* This work has been supported by the National Natural Science Foundation of China (Nos.61405178 and 61505176), and the Zhejiang Provincial Key Natural Science Foundation of China (No.LZ21F010001).

** E-mail: 119029@zust.edu.cn

coupling between the core mode and the cladding mode. From the coupled-mode theory, we know that there is a total power conversion length (TPCL) for an LPFG with a constant grating period at the phase-matched wavelength, where the core mode couples 100% of the power to the phase-matched cladding mode[1]. However, for a CLPFG with a varying period, it's hard to ensure that the effective coupling length for each phase-matched wavelength is equal to the TPCL, because of the dispersion in optical fibers. When the effective coupling length is less than the TPCL, the core mode cannot couple 100% of the power to the cladding mode. When the effective coupling length is greater than the TPCL, the power coupled to the cladding mode will couple back to the core mode. Both of these cases would induce a low coupling efficiency, and fluctuations appear on the attenuation band.

Based on the above analysis, in this paper we propose a method by using a high refractive index (RI) coated CLPFG to increase the coupling efficiency and achieve an ultra-broadband filter. When the CLPG is coated with high RI material, guided cladding modes in the CLPFG will turn into leaky ones and the core mode will couple with these leaky modes instead of guided cladding modes[20]. Because of leakage, the power coupled to these leaky modes from the core mode will radiate out of the fiber and cannot be recoupled back to the core mode, which resolves the conflict between effective coupling length and the TPCL, making a filter with both high efficiency and compact structure possible. With this method, an ultra-broadband filter with high efficiency can be achieved by simply coating the CLPFG with high RI material, instead of resorting to other complicated techniques, such as apodization[12].

Fig.1(a) shows the theoretical model of the CLPFG coated by a material whose RI (n_s) is higher than that of the cladding, and Fig.1(b) shows the corresponding RI profile of a reference fiber, where n_{co} and n_{cl}, r_{co} and r_{cl} are the RIs and radii of the core and cladding, respectively. The thickness of the coating is assumed to be large enough for the effect of air on the fiber modes to be neglected. Moreover, since the coating RI is higher than that of the cladding, guided cladding modes of the reference fiber do not experience total internal reflection and thus turn into leaky modes[20]. In our simulation, leaky modes in the reference fiber, which is referred to as a leaky or hollow dielectric waveguide[21], were solved by making use of an equivalent model terminated by a perfect electric conductor-backed perfectly matched layer (PEC-backed PML)[22], and the coupling between guided core mode and leaky modes was analyzed by a unified complex coupled-mode analysis[23].

For a uniform LPFG with a constant grating period, the complex coupled-mode equation describing the coupling between core mode and a phased matched leaky mode can be expressed as[23]

$$\begin{cases} \dfrac{\mathrm{d}A_1}{\mathrm{d}z} = -\mathrm{j}K_{11}A_1 - \mathrm{j}\dfrac{v}{2}K_{1n}A_n\mathrm{e}^{\mathrm{j}2\Delta\beta_n z} \\ \dfrac{\mathrm{d}A_n}{\mathrm{d}z} = -\mathrm{j}\dfrac{v}{2}K_{n1}A_1\mathrm{e}^{-\mathrm{j}2\Delta\beta_n z} \end{cases}, \tag{1}$$

where A_1 and A_n are the amplitudes of core mode and nth leaky mode in the reference fiber, respectively, and K_{11} and K_{n1} are the self-coupling coefficient and cross-coupling coefficient, respectively. It should be noted that K_{n1} is a complex number, but its imaginary part was ignored in the following analysis and simulations because of its small magnitude and negligible contributions to the coupling process. v is the fringe visibility of the index change. $\Delta\beta_n$ is the phase detuning factor and defined as

$$\Delta\beta_n = \frac{1}{2}(\beta_1 - \beta_n - \frac{2\pi}{\Lambda}), \tag{2}$$

where Λ is the period of the LPFG, and β_1 and β_n are the propagation constants of the core mode and nth leaky mode, respectively.

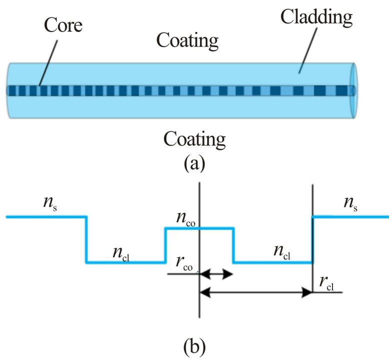

Fig.1 (a) Theoretical model of the coated CLPFG; (b) RI profile of the reference fiber

As β_n is a complex number due to the leakage property of the nth leaky mode, $\Delta\beta_n$ is complex and can be rewritten as $\Delta\beta_n=\Delta\beta+\mathrm{j}\Delta\alpha$. Here, $\Delta\alpha=-\mathrm{Im}(\beta_n)/2$, since the propagation constant of the guided core mode β_1 is real.

To solve Eq.(1), a parameter transformation was used as follows

$$\begin{cases} E_1 = A_1\mathrm{e}^{-\mathrm{j}(\Delta\beta-\frac{K_{11}}{2})z} \\ E_n = A_n\mathrm{e}^{\mathrm{j}(\Delta\beta+\frac{K_{11}}{2})z}\mathrm{e}^{-2\Delta\alpha z} \end{cases}. \tag{3}$$

Then, Eq.(3) was inserted into Eq.(1) and the coupled first order differential equation group was turned into a second order differential equation only on E_1, deriving

$$\begin{cases} \dfrac{\mathrm{d}^2E_1}{\mathrm{d}z^2} + 2\Delta\alpha\dfrac{\mathrm{d}E_1}{\mathrm{d}z} + C^2E_1 = 0 \\ E_1(0)=1, \quad \dfrac{\mathrm{d}E_1}{\mathrm{d}z}\Big|_{z=0} = 0 \end{cases}, \tag{4}$$

where the phase matching condition is

$$\delta = \frac{K_{11}}{2} + \Delta\beta = 0, \tag{5}$$

and the initial conditions $E_1(0)=1$ and $E_n(0)=0$ were used.

$\frac{\nu}{2}K_{1n}$ was replaced by C in Eq.(4) for simplicity of the expression.

The analytical solution of Eq.(4) could be derived easily, and from this it was possible to deduce how coupling with the leaky mode led to the evolution of the core mode power. As Eq.(4) has a similar form to that of the damped oscillations, the evolution of the core mode power could further be explicitly categorized into three cases by an analogy, which is illustrated in Fig.2. When $\Delta\alpha<C$, the core mode power transmits periodically along the coupling length with an attenuation, which corresponds to the under-damped state of damped oscillations. When $\Delta\alpha>C$, the core mode attenuates monotonously, which corresponds to the over-damped state of damped oscillations. When $\Delta\alpha=C$, the core mode attenuates monotonously, too, but with a higher attenuation rate, it corresponds to the critically-damped state of damped oscillations. Consequently, to achieve a desired coupling efficiency with a short coupling length, the value of $\Delta\alpha/C$ needed to be set at around 1, where the core mode power attenuated monotonously and most rapidly. In addition, the value of $\Delta\alpha/C$ less than 1 is preferable to the value of $\Delta\alpha/C$ greater than 1, as the core mode power attenuates more rapidly in this case.

The analysis of core mode and leaky mode coupling in a uniform LPFG showed clearly how the complex propagation constant of the leaky mode affected the evolution of the core mode power. It also provided a way to optimize an ultra-broadband filter based on a CLPFG.

For the CLPFG, which had a varying period, the corresponding complex coupled mode equation had the same form as Eq.(1), but with a varying phase detuning factor $\Delta\beta_n$. Because of the varying $\Delta\beta_n$, it was difficult to solve Eq.(1) as done for the uniform LPFG. The transmission characteristics of the CLPFG were analyzed using the transfer matrix method, where the CLPFG was divided into N sections and each section was regarded as a uniform LPFG. Therefore, the transmission properties of the core mode for each section were the same as that in Fig.2. The transmission spectrum of CLPFG can be considered as a superposition of the N spectra of N uniform LPFGs.

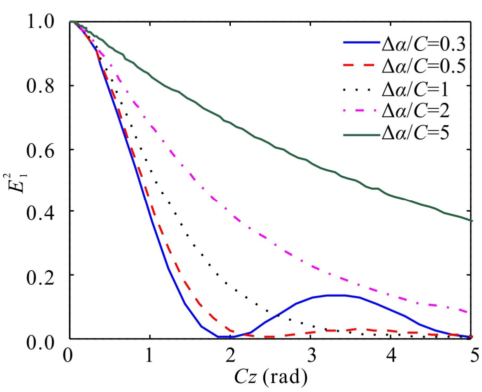

Fig.2 Variations of the core mode power with the coupling length for different $\Delta\alpha/C$ values

Simulations of the coated CLPFG were based on the theoretical analysis above. The parameters were r_{co}=2.5 μm, r_{cl}=62.5 μm, n_{co}=1.458, n_{cl}=1.45, and $\nu=10^{-3}$. First, with the phase matching condition indicated by Eq.(5), PMCs for core mode and leaky modes were calculated as shown in Fig.3, which clearly revealed the relationship between resonant wavelength and grating period. Fig.3 gives the PMCs only for several higher-order leaky modes. PMCs for lower-order modes overlapped with their neighboring ones and we had to take numerous leaky modes in the analysis, which made the design of an ultra-broadband filter complicated, hence higher-order leaky modes were preferable. As shown in Fig.3, if the period of PMTP was set as the maximum grating period of CLPFG, the attenuation band of the CLPFG broadened both to longer wavelength and to shorter wavelength as the grating period decreased. As a result, the grating period change required for a broadband filter will decrease dramatically by taking advantage of PMTP. This property is similar to that of coupling with guided cladding modes[12]. In addition, if the maximum grating period of CLPFG is set at the PMTP, the central wavelength of the attenuation band of the CLPFG-based filter corresponds to the resonant wavelength at PMTP, and the minimum grating period is determined by the bandwidth of the filter. Taking the $HE_{1,13}$ leaky mode as an example, to achieve a design bandwidth of 400 nm, the grating period range is from 139.5 μm to 142.5 μm, as marked by the dashed lines in Fig.3. Furthermore, within this range, only the $HE_{1,13}$ mode has the chance to fulfill the phase matching condition with the core mode. Therefore, only the $HE_{1,13}$ leaky mode needs to be considered in the coupled mode equation, which greatly simplifies the analysis.

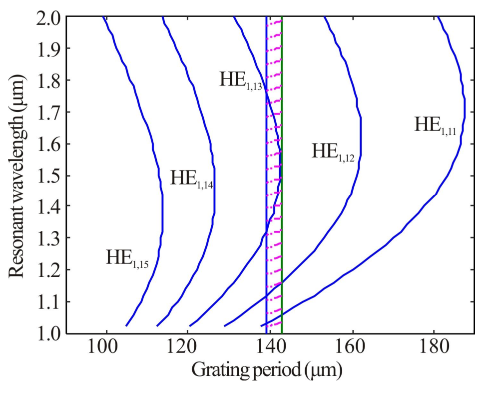

Fig.3 Phase matching curves of higher order leaky modes

Besides the grating period change, another parameter that needed to be considered for a coated CLPFG-based broadband filter was the coating RI, n_s. In the simulation of PMCs in Fig.3, the coating RI was set to be 1.55. In fact, as the real part of the propagation constant of leaky mode was insensitive to n_s[20], PMCs which were determined by the real part of the propagation constant would be the same for various n_s, as long as $n_s>n_{cl}$. By contrast, the imaginary part of the leaky mode propagation constant depended strongly on the coating RI. As the core mode attenuation rate was strongly affected by the imaginary part of the leaky mode propagation constant, as shown in Fig.2, the coupling efficiency between core mode and leaky mode could thus be improved by careful selection of the coating RI.

The variations of $\Delta\alpha/C$ for the $HE_{1,13}$ leaky mode with wavelengths at different n_s were given in Fig.4. We can see that the value of $\Delta\alpha/C$ is larger for longer wavelengths, which results from the weaker restriction of light for a fiber operating at longer wavelength. In addition, the value of $\Delta\alpha/C$ decreases when increasing n_s at the same wavelength. This is because the leaky modes are formed by partial reflection from the interface of cladding and coating, when the coating RI increases, leaky modes are better confined, leading to a smaller $\Delta\alpha$.

To achieve a high coupling efficiency between the core mode and leaky mode, 1.59 was selected from the four simulated cases in Fig.4, under which the value of $\Delta\alpha/C$ ranged from 0.6 to 1.2 for a design bandwidth of 400 nm. However, it should be noted that, from Fig.4 we can only roughly determine a comparatively optimal coating RI for the design, as the variations of $\Delta\alpha/C$ with n_s is continuous and $\Delta\alpha/C$ is a range for the ultra-broad design bandwidth. Further improvement of coating RI can be taken through the simulated spectra of the CLPFG.

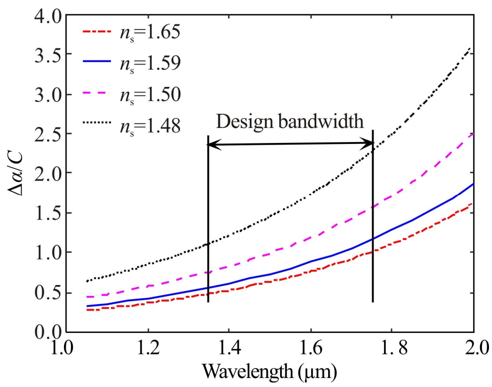

Fig.4 Variations of $\Delta\alpha/C$ with wavelength for different n_s values

Using these parameters, the transmission spectrum of the CLPFG with a length of 3.5 cm was simulated and was shown by the solid line in Fig.5. We can see that the attenuation band is symmetrical, and the bandwidth coincides with that designed based on PMCs in Fig.3. However, there was a small peak at the center of the attenuation band, as can be seen in Fig.5. As a flat attenuation band is more desirable in practice, this small peak should be eliminated.

As the center of the attenuation band corresponds to the resonant wavelength of the maximum grating period, where the efficient coupling length between core mode and leaky mode is shorter compared with other wavelengths, this small peak appears. To increase the efficient coupling length at the center of the attenuation band, the maximum grating period should be expanded. Through simulation analysis, 143.2 μm was determined as the expanded maximum grating period. Meanwhile, the minimum grating period was expanded to 139.2 μm to achieve desired attenuation at the two ends of the attenuation band. The transmission spectrum for the expanded grating period range is shown by the dashed line in Fig.5, a flat but still symmetrical attenuation band is achieved. Additionally, the transmission spectra of the CLPFG with different coating RI around 1.59 was also given in Fig.5, it can be seen that when n_s is greater than or less than 1.59, the attenuation in lower wavelength range increases or decreases, respectively. In view of flatness of the attenuation band, the coating RI of 1.59 is preferable and the corresponding spectrum is replotted in Fig.6, as shown by the dashed line, to describe its operating bandwidth and flatness concisely. It needs to be noted that, as flatness within the operating bandwidth is also a key measure for the performance of a filter, we suggest the central part of the attenuation band with flatness less than 2.5 dB be the operating bandwidth for practical applications, as indicated in Fig.6. What's more, the transmittance of the core mode within the operating bandwidth is lower than 0.1%.

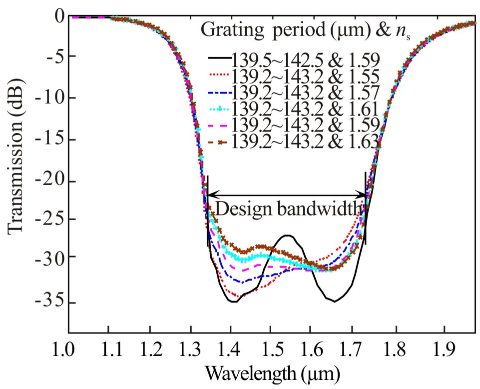

Fig.5 Transmission spectra of the CLPFG

Furthermore, to examine the robustness of the coated CLPFG-based filter, we investigated the influence of temperature on its transmission spectra. As the optimal RI of the coating is 1.59, polystyrene (PS) is a preferred material that can be used as the coating[24]. PS has small absorption in optical communication band and good compatibility with optical fiber, besides, its RI is just 1.59 at room temperature[24]. The thermo-optic coefficients of PS and silica are -1.2×10^{-4}/°C and 8.3×10^{-6}/°C, respectively[24,25]. The thermal expansion coefficients of PS and silica are 2.2×10^{-4}/°C and 1.1×10^{-6}/°C[24,25], respectively. With these parameters, the variation of transmission spectra of the coated CLPFG-based filter with temperature was simulated, as shown in Fig.6. It can be seen that when the temperature changes from 0 °C to 80 °C, the transmission spectra has only slight change with loss, while the central wavelength and operating bandwidth are nearly unchanged, proving the robustness of the filter. This phenomenon is quite different with that of the uncoated LPFG[3], because the coupling, in high RI coated fiber grating, is between core mode and leaky modes, and the phase constant of leaky mode is insensitive to the coating RI[20].

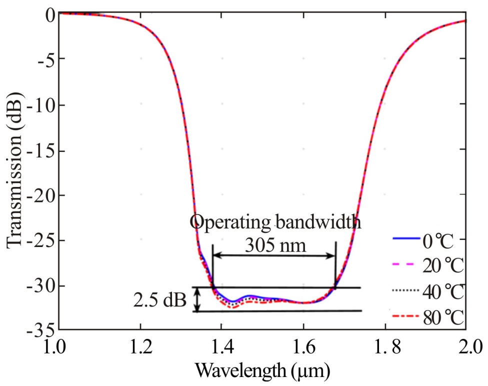

Fig.6 Transmission spectra of the CLPFG under various temperatures

To further show the design mechanism, the transmission of the core mode along the coupling length for different wavelengths is shown in Fig.7, with grating period range from 139.2 μm to 143.2 μm. The wavelengths of 1.34 μm and 1.72 μm correspond to the edge of the design bandwidth, where the transmission loss of the core mode is 25 dB. Moreover, the core mode power attenuated basically monotonously along the coupling length, which is the basic reason for achieving this compact ultra-broadband CLPFG-based filter without using apodization technique. The monotonous attenuation of core mode power along the coupling length was quite different from that of coupling with cladding modes, where periodic power exchange is observed[1,2]. Additionally, we can see that each curve had a sharp drop where the phase matching condition was closely fulfilled.

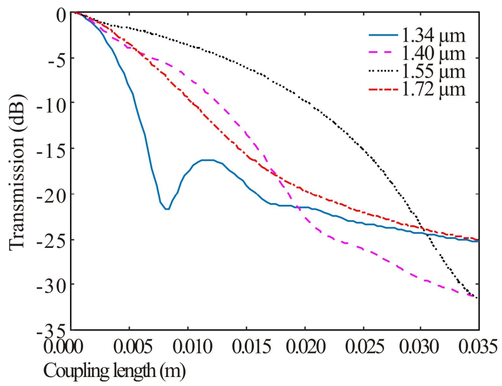

Fig.7 Transmission spectra of the core mode along the coupling length at different wavelengths

An ultra-broadband fiber filter based on a coated CLPFG was proposed and demonstrated by simulations. The RI of the coating material over CLPFG was chosen to be higher than that of the fiber cladding, to introduce the coupling of core mode with leaky modes. Because of leakage, the power coupled to the leaky modes from core mode will leak out of the fiber and cannot be recoupled back to the core mode, which is desired for a high coupling efficiency. The coupling between core mode and leaky mode was analyzed with complex coupled-mode theory. The core mode power evolution resulting from coupling with leaky modes was revealed, and the conditions in which the core mode power attenuates the most quickly were identified. In addition, the PMTP was used in the design, which can help to resolve the conflict between the range of grating period change and the grating length in the CLPFG.

Based on the theoretical analysis, simulations were done. The $HE_{1,13}$ leaky mode was used as an example, and a filter with a bandwidth of over 300 nm, an attenuation loss over 30 dB, a flatness of less than 2.5 dB and a length of 3.5 cm was demonstrated, exhibiting both a high coupling efficiency and a wide symmetrical attenuation band. The CLPFG-based filter is simple in structure, easy to be fabricated and compact in size, it will be promising in the applications of optical communications and sensing.

In the design of this filter, we took advantage of the unidirectional coupling from the core mode to leaky modes as well as the small period range requirement for a large band at PMTP. Because of the unidirectional coupling, a high coupling efficiency can be achieved by carefully selecting the coating material of the CLPFG, instead of resorting to other techniques, such as apodization[12]. The coupling property with leaky mode illustrated and the designing idea proposed in this paper may inspire the design of other fiber-based devices.

Statements and Declarations

The authors declare that there are no conflicts of interest related to this article.

References

[1] ERDOGAN T. Cladding-mode resonances in short- and long-period fiber grating filters[J]. Journal of the Optical Society of America A-optics image science and vision, 1997, 14(8)：1760-1773.

[2] VENGSARKAR A M, LEMAIRE P J, JUDKINS J B, et al. Long-period fiber gratings as band-rejection filters[J]. Journal of lightwave technology, 1996, 14(1)：58-65.

[3] BHATIA V, VENGSARKAR A M. Optical fiber long-period grating sensors[J]. Optics letters, 1996, 21(9)：692-694.

[4] YANG Y, CAO Y, CHEN X. A study on relation between ultra-wideband filtering characteristics and structural parameters for a chirped long-period fiber grating[J]. Indian journal of physics, 2013, 87(3)：297-302.

[5] HE T, DEMAS J, RAMACHANDRAN S. Ultra-low loss dispersion control with chirped transmissive fiber gratings[J]. Optics letters, 2017, 42(13)：2531-2534.
[6] ZHANG S, GENG T, WANG S J, et al. High-sensitivity strain and temperature simultaneous measurement sensor based on multimode fiber chirped long-period grating[J]. IEEE sensors journal, 2020, 20(24)：14843-14849.
[7] ISRAELSEN S M, ROTTWITT K. Broadband higher order mode conversion using chirped microbend long period gratings[J]. Optics express, 2016, 24(21)：23969-23976.
[8] JIANG H P, GU Z T, WU J Y. Design of high sensitivity refractive index sensor based on small chirp coefficient LPFG[J]. Optical and quantum electronics, 2022, 54(6)：343.
[9] ZHANG S, GENG T, NIU H W, et al. All fiber compact bending sensor with high sensitivity based on a multimode fiber embedded chirped long-period grating[J]. Optics letters, 2020, 45(15)：4172-4175.
[10] YANG Y, GU Z T. Ultra-wideband filtering characteristics of chirped long-period fiber gratings with apodization optimization[J]. Acta optica sinica, 2012, 32(10)：1006006.
[11] YANG Y, GU Z T. Single-channel broadband and multichannel narrowband filtering characteristics of linear chirped long-period fiber gratings[J]. Optical engineering, 2014, 52(11)：116101.
[12] FENG W, GU Z T. Ultra-broadband optical filter based on chirped long-period fiber grating and PMTP[J]. IEEE photonics technology letters, 2018, 30(15)：1361-1363.
[13] LI Z Y, GU Z T, LING Q, et al. Design of an ultra-broadband optical filter based on a local micro-structured long period fiber grating near PMTP[J]. Applied optics, 2022, 61(14)：3965-3971.
[14] ZHOU W, RAN Y L, YAN Z J, et al. Sensitivity characterization of cascaded long-period grating operating near the phase-matching turning point[J]. Sensors, 2020, 20(21)：5978.
[15] WU W Y, GU Z T, LING Q. High-sensitivity few-mode long-period fiber grating refractive index sensor based on mode barrier region and phase-matching turning point[J]. Optics communications, 2020, 473：125997.
[16] ZHENG Y, GUO H Y, FENG M, et al. Wavelength-tunable, ultra-broadband, biconical, long-period fiber grating mode converter based on the dual-resonance effect[J]. Sensors, 2021, 21(17)：5970.
[17] REN K L, CHENG M H, REN L Y, et al. Ultra-broadband conversion of OAM mode near the dispersion turning point in helical fiber gratings[J]. OSA continuum, 2020, 3(1)：77-87.
[18] KOPP V I, CHURIKOV V M, SINGER J, et al. Chiarl fiber gratings[J]. Science, 2004, 305(5680)：74-75.
[19] ZHAO H, LI H P. Advances on mode-coupling theories, fabrication techniques, and applications of the helical long-period fiber gratings：a review[J]. Photonics, 2021, 8(4)：106.
[20] STEGALL D B, ERDOGAN T. Leaky cladding mode propagation in long-period fiber grating devices[J]. IEEE photonics technology letters, 1999, 11(3)：343-345.
[21] MARCUSE D. Theory of dielectric optical waveguides[M]. New York：Academic Press, 1974.
[22] LU Y C, YANG L, HUANG W P, et al. Improved full-vector finite-difference complex mode solver for optical waveguides of circular symmetry[J]. Journal of lightwave technology, 2008, 26(13)：1868-1876.
[23] YANG L, XUE L L, LU L Y, et al. New insight into quasi leaky mode approximations for unified coupled-mode analysis[J]. Optics express, 2010, 18(20)：20595-20609.
[24] SALUNKHE T T, LEE D J, LEE H K, et al. Enhancing temperature sensitivity of the Fabry-Perot interferometer sensor with optimization of the coating thickness of polystyrene[J]. Sensor, 2020, 20(3)：794.
[25] TAKAHASHI S, SHIBATA S. Thermal variation of attenuation for optical fibers[J]. Journal of non-crystalline solids, 1979, 30(3)：359-370.